International Journal of Civil and Structural Engineering – IJCSE 2018
Copyright © Institute of Research Engineers and Doctors , SEEK Digital Library
Volume 5 : Issue 1- [ISSN : 2372-3971] - Publication Date: 25 June, 2018

Assessing wind induced stay vibrations in bridges

Pietro Croce, Paolo Formichi, Filippo Landi, Roberto Castelluccio

Abstract—**Stay vibration events have been reported all over the world on cable-stayed bridges. Cable vibrations cause bridge users discomfort and may also lead to bridge collapse. Aim of this study is to investigate relevant cable vibration phenomena directly induced by wind, such as buffeting, von Kármán vortex-shedding, dry inclined galloping and rain wind induced vibrations. The results are presented in terms of required necessary damping to control the dynamic stability of stays for a significant case study.**

Keywords—**cable-stayed bridge, cable vibrations, aerodynamics, bluff bodies**

I. Introduction

Cable-stayed bridges became very popular during the second half of the twentieth century. There are four main reasons that lead to an enormous increase in the construction of cable-stayed bridges [1]: cable-stayed bridges are stiffer than suspension bridges, they are adequate for construction in weak soil due to their self-balancing features, they are economically advantageous for moderate to large spans and they have remarkable aesthetic qualities. Moreover, recent improvements in cable technology and in erection techniques allows to design increasingly large and slender cable-stayed bridges; considering in addition that stay cables are very flexible elements, with small damping coefficients ($\xi \leq 0.50\%$) it is clear that these elements are very vulnerable to vibrations under dynamic loads.

Cable vibrations alarm bridge users (especially pedestrian users) with a subsequent discomfort, but these can also cause a fatigue damage. The first significant report on cable vibration dates back to 1976 [2]: in effect, during the erection of the Brotonne bridge (France) longer cables hit each other, due to vibrations, and the problem was solved mounting viscous dampers close to the deck anchorages [1]. In the subsequent years many vibration problems occurred in bridges all over the world and then started an intensive research on this issue.

Relevant cable vibration phenomena induced by wind are discussed here, referring to a significant case study.

II. Cable vibration phenomena directly induced by wind

Among cable vibration phenomena directly induced by wind, there are *Buffeting*, *von Kármán Vortex-Shedding* and *Dry Inclined Galloping:* the first refers to forced vibrations caused by unsteady wind gusts, the second is characterized by an alternate shedding of vortices at the top and bottom surfaces of cables and the third is an aeroelastic phenomenon typical of yawed circular stay, where the appearance of an axial flow behind cables for certain yawing angles alters the section radial symmetry. Then there are *Rain-Wind Induced Vibrations*: under combination of rain and wind, oscillating rivulets form at the upper and lower surfaces of the cable altering section radial symmetry (Fig. 1).

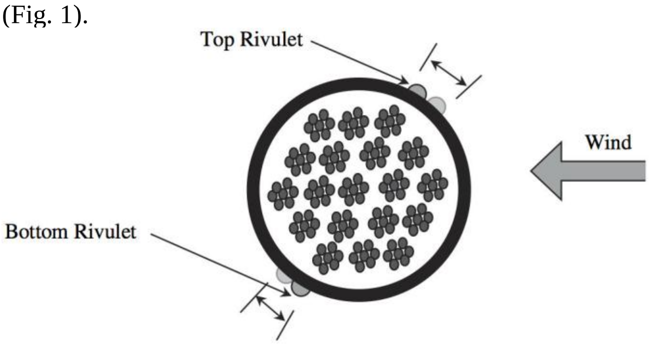

Figure 1. Cross section of a cable with upper and lower rivulet, from [3]

In these cases an aerodynamic instability is possible, due to symmetry loss. Indeed, when the angle of attack β of the wind is small ($\beta \approx 0$), the so-called classical Den Hartog [4] necessary condition for incipient galloping instability is

$$\left(\frac{\mathrm{d}C_{\mathrm{L}}}{\mathrm{d}\beta} + C_{\mathrm{D}} \right)_{\beta \approx 0} < 0 \tag{1}$$

where C_{L} is the lift coefficient and C_{D} is the drag coefficient. Obviously, circular cross sections are never subjected to galloping, as the variation of C_{L} is always null, due to symmetry, and drag coefficient (C_{D}) is always positive.

When (1) is satisfied, the overall system damping (d) may be negative because aerodynamic damping becomes negative:

$$d = 2m\omega\xi + \frac{1}{2}\rho U D \left(\frac{\mathrm{d}C_{\mathrm{L}}}{\mathrm{d}\beta} + C_{\mathrm{D}} \right)_{\beta \approx 0} \tag{2}$$

being m the cable mass per unit length, ω the natural circular frequency, ξ the damping ratio, $\rho = 1.2\ \mathrm{kg/m^3}$ the air density at 20°C, U is the uniform wind velocity and D is the diameter of the cable.

III. The case study

Wind induced vibrations are assessed here referring to a cable-stayed bridge crossing the river Arno in Figline Valdarno, a town near Florence [5]. This self-anchored cable-stayed bridge has a total length of 281 m with three spans respectively of 44 m, 37 m and 200 m (Fig. 2). The S355 steel box girder has a trapezoidal cross section, 2.00 m depth and 14.96 m width (Fig. 3). The 12 mm thick orthotropic steel deck is reinforced with trapezoidal stiffeners spaced 600 mm center to center.

Pietro Croce, Paolo Formichi, Filippo Landi, Roberto Castelluccio
University of Pisa, Department of Civil and Industrial Engineering - Structural Division
Italy

International Journal of Civil and Structural Engineering – IJCSE 2018
Copyright © Institute of Research Engineers and Doctors , SEEK Digital Library
Volume 5 : Issue 1- [ISSN : 2372-3971] - Publication Date: 25 June, 2018

The deck is suspended to a pylon via 17 pairs of locked-coil strands forming an asymmetric semi-fan; these cables are 15.00 m spaced on the girder and 3.75 m on the pylon. The concrete A-shaped pylon has a total height of 96.00 m. All substructures are founded on piles with a diameter of 1.60 m.

Structural analysis was carried out with SAP2000®.

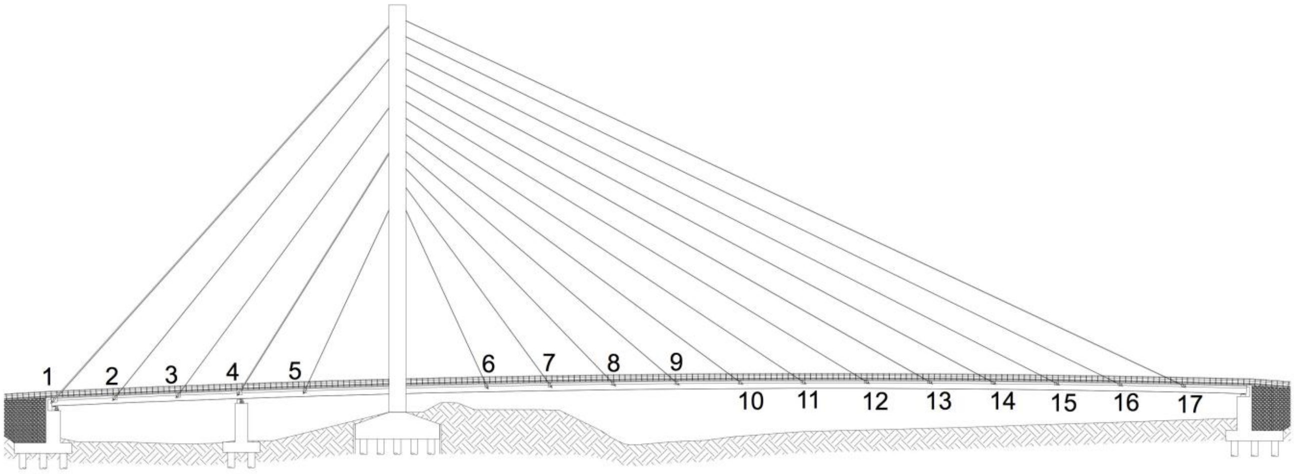

Figure 2. The cable-stayed bridge analyzed

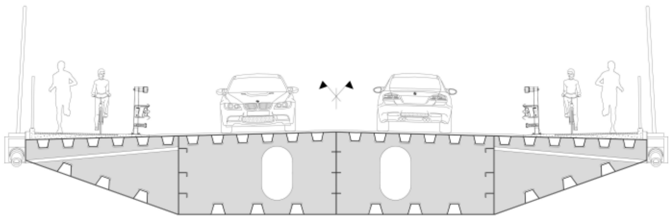

Figure 3. The bridge deck.

IV. Case study analysis

A. Natural frequencies of cables

The n-th cable circular frequency can be evaluated with Mehrabi and Tabatabai formula [6],

$$\omega_n = \frac{\pi n}{l}\sqrt{\frac{T}{m}}\left(\alpha\,\beta_n - 0.24\frac{\mu}{\zeta}\right), \tag{3}$$

where sag and bending stiffness effects are introduced in vibrating chord theory by means of the dimensionless coefficients α, β_n, μ and ζ [6]:

$$\alpha = 1 + 0.039\,\mu \tag{4}$$

$$\beta_n = 1 + \frac{2}{\zeta} + \frac{4 + \frac{n\,\pi^2}{2}}{\zeta^2} \tag{5}$$

$$\zeta = \sqrt{\frac{T\,l^2}{E\,J}}\,; \tag{6}$$

T is the component of cable tension along cable chord in the dead load configuration;

l is the horizontal projection of cable;

E is Young's modulus of cable material;

J is the 2nd area moment of cable cross section;

μ is a coefficient varying with n:

$\mu = \lambda^2$ if $n = 1$

$\mu = 0$ if $n > 1$ (in-plane modes)

$\mu = 0$ for out-of-plane modes.

λ^2 is a parameter, introduced by Irvine [7], including both the geometric and deformational characteristics of a suspended cable and defined as

$$\lambda^2 = \left(\frac{m\,g\,L}{T}\right)^2 \frac{L}{L_e}\frac{E\,A_0}{T} \tag{7}$$

where

L is the chord length;

A_0 is the area of undeformed cable cross section;

L_e is a virtual length of cable, defined by

$$L_e = \int_0^L \left(\frac{ds}{dx}\right)^3 dx\,; \tag{8}$$

International Journal of Civil and Structural Engineering – IJCSE 2018
Copyright © Institute of Research Engineers and Doctors , SEEK Digital Library
Volume 5 : Issue 1- [ISSN : 2372-3971] - Publication Date: 25 June, 2018

f is the cable sag at midpoint.

As known, for shallow cables ($f/L \leq 1/8$) the *catenary* can be approximated by an *elastic parabola*, so

$$L_\mathrm{e} \approx L\left[1+8\left(\frac{f}{L}\right)^2\right] \tag{9}$$

$$f = \frac{m\,g\,L^2}{8T}\,. \tag{10}$$

The accuracy of (3) is higher for cables with $\zeta \geq 50$ and $\lambda^2<3.1$: if $\zeta<50$ bending stiffness can be disregarded, if $\lambda^2 \geq 3.1$ cables are relatively flabby and vibrating chord theory is not acceptable.

Table I and Table II show the Irvine parameter and fundamental frequencies (in-plane and out-of-plane) of stays.

TABLE I. IRVINE PARAMETER OF STAYS.

Stay	T (kN)	θ (°)	m (kg/m)	L (m)	l (m)	f (m)	L_e (m)	A_0 (m^2)	E (kN/m^2)	λ^2 (–)
1	7335	48	300	122	81	0.750	122	0.037 40	1.8×10^8	2.211
2	942	51	17	106	66	0.247	106	0.002 09	1.8×10^8	0.138
3	798	54	17	88	51	0.198	88	0.002 09	1.8×10^8	0.154
4	10 318	58	300	69	36	0.172	69	0.037 40	1.8×10^8	0.256
5	964	66	20	52	21	0.069	52	0.002 49	1.8×10^8	0.052
6	965	65	24	51	22	0.078	51	0.002 92	1.8×10^8	0.081
7	707	54	24	62	37	0.156	62	0.002 92	1.8×10^8	0.302
8	821	46	24	74	52	0.193	74	0.002 92	1.8×10^8	0.278
9	971	40	27	88	67	0.264	88	0.003 39	1.8×10^8	0.365
10	1062	37	27	102	82	0.325	102	0.003 39	1.8×10^8	0.375
11	1123	34	27	116	97	0.401	116	0.003 39	1.8×10^8	0.414
12	1334	31	31	131	112	0.493	131	0.003 89	1.8×10^8	0.476
13	1383	30	31	146	127	0.589	146	0.003 89	1.8×10^8	0.530
14	1428	28	31	161	142	0.694	161	0.003 89	1.8×10^8	0.585
15	1500	27	31	176	157	0.791	176	0.003 89	1.8×10^8	0.605
16	1499	26	31	191	172	0.935	191	0.003 89	1.8×10^8	0.715
17	1628	25	27	206	187	0.872	206	0.003 39	1.8×10^8	0.429

TABLE II. FUNDAMENTAL CIRCULAR FREQUENCIES OF STAYS.

Stay	D (mm)	J (m^4)	ζ (–)	μ (–)	α (–)	β_1 (–)	$\omega_{1,\mathrm{in}}$ (rad/s)	$\omega_{1,\mathrm{out}}$ (rad/s)
1	230	1.17×10^{-4}	52.22	2.211	1.086	1.042	4.50	4.18
2	55	3.82×10^{-7}	266.95	0.138	1.005	1.008	7.09	7.06
3	55	3.82×10^{-7}	190.09	0.154	1.006	1.011	7.94	7.90
4	230	1.17×10^{-4}	27.66	0.256	1.010	1.084	9.17	9.09
5	60	5.41×10^{-7}	72.90	0.052	1.002	1.029	13.70	13.68
6	65	7.45×10^{-7}	63.17	0.081	1.003	1.034	12.93	12.90
7	65	7.45×10^{-7}	91.44	0.302	1.012	1.023	9.12	9.02
8	65	7.45×10^{-7}	138.82	0.278	1.011	1.015	8.11	8.03
9	70	1.00×10^{-6}	167.94	0.365	1.014	1.012	6.95	6.85
10	70	1.00×10^{-6}	215.13	0.375	1.015	1.009	6.25	6.16
11	70	1.00×10^{-6}	261.83	0.414	1.016	1.008	5.63	5.54
12	75	1.32×10^{-6}	287.15	0.476	1.019	1.007	5.08	4.99
13	75	1.32×10^{-6}	331.64	0.530	1.021	1.006	4.65	4.56
14	75	1.32×10^{-6}	376.89	0.585	1.023	1.005	4.29	4.20
15	75	1.32×10^{-6}	427.17	0.605	1.024	1.005	4.02	3.93
16	75	1.32×10^{-6}	467.90	0.715	1.028	1.004	3.71	3.61
17	70	1.00×10^{-6}	608.67	0.429	1.017	1.003	3.80	3.74

B. *Buffeting*

In most circumstances *buffeting* is restrained from aerodynamic damping that is proportional to the uniform wind velocity both in along-wind direction, (11), and in across-wind direction, (12).

$$\xi_{\mathrm{aer,kD}} = \frac{\rho U\,D C_\mathrm{D}}{2m\omega_k} \tag{11}$$

$$\xi_{\mathrm{aer,kL}} = \frac{\rho U\,D C_\mathrm{D}}{4m\omega_k} \tag{12}$$

Drag coefficient for a circular section varies with the Reynolds Number, $Re=UD/\nu$, where ν is the kinematic viscosity of the air, whose value at 20°C is 0.15 cm^2/s. In the supercritical region ($Re>10^6$), it results $C_\mathrm{D}=0.7$. The reference wind velocity (return period of 50 years) for construction site is 27 m/s (97 kmph). Table III shows that, for this case, along-wind aerodynamic damping is in the range (0.05÷0.45)% considering U=15 m/s=54 kmph.

TABLE III. ALONG-WIND AERODYNAMIC DAMPING.

Stay	D (mm)	m (kg/m)	$\omega_{1,\mathrm{in}}$ (rad/s)	$U=15\,\mathrm{m/s}$ Re (–)	C_D (–)	$\xi_{\mathrm{aer,1D}}$ (%)	$U=30\,\mathrm{m/s}$ Re (–)	C_D (–)	$\xi_{\mathrm{aer,1D}}$ (%)
1	230	300	4.50	2.3×10^8	0.7	0.11	4.6×10^8	0.7	0.21
2	55	17	7.09	5.5×10^7	0.7	0.29	1.1×10^8	0.7	0.58
3	55	17	7.94	5.5×10^7	0.7	0.26	1.1×10^8	0.7	0.52
4	230	300	9.17	2.3×10^8	0.7	0.05	4.6×10^8	0.7	0.11
5	60	20	13.70	6.0×10^7	0.7	0.14	1.2×10^8	0.7	0.28
6	65	24	12.93	6.5×10^7	0.7	0.13	1.3×10^8	0.7	0.27
7	65	24	9.12	6.5×10^7	0.7	0.19	1.3×10^8	0.7	0.38
8	65	24	8.11	6.5×10^7	0.7	0.21	1.3×10^8	0.7	0.43
9	70	27	6.95	7.0×10^7	0.7	0.23	1.4×10^8	0.7	0.47
10	70	27	6.25	7.0×10^7	0.7	0.26	1.4×10^8	0.7	0.52
11	70	27	5.63	7.0×10^7	0.7	0.29	1.4×10^8	0.7	0.58
12	75	31	5.08	7.5×10^7	0.7	0.30	1.5×10^8	0.7	0.59
13	75	31	4.65	7.5×10^7	0.7	0.32	1.5×10^8	0.7	0.65
14	75	31	4.29	7.5×10^7	0.7	0.35	1.5×10^8	0.7	0.70
15	75	31	4.02	7.5×10^7	0.7	0.38	1.5×10^8	0.7	0.75
16	75	31	3.71	7.5×10^7	0.7	0.41	1.5×10^8	0.7	0.81
17	70	27	3.80	7.0×10^7	0.7	0.43	1.4×10^8	0.7	0.85

These values are consistent with literature values obtained from field observations [1]. Notice that $\xi_{\mathrm{aer,kD}}=2\,\xi_{\mathrm{aer,kL}}$ so vibrations often occur in the plane of cables.

C. *von Kármán Vortex-Shedding*

The shedding frequency of vortices is governed by the *Strouhal law*:

$$f_\mathrm{v} = \frac{U\,St}{D}. \tag{13}$$

Strouhal number (St) varies with the shape of cable cross section and on circular cylinder $St=0.2$ for $10^5 \leq Re \leq 10^7$ [8]. Provided that *lock-in* cannot occur, i.e. f_v (13) is sufficiently far to some cable frequencies to exclude *synchronization* between these frequencies, producing additional across-wind loads, this linear law applies to *Scruton number*

$$Sc = \frac{2\delta m_\mathrm{e}}{\rho D^2} > 20\,, \tag{14}$$

where

$$\delta = \ln \frac{a_n}{a_{n+1}} = \frac{2\pi\xi}{\sqrt{1-\xi^2}} \approx 2\pi\xi \qquad (15)$$

is the logarithmic decrement of structural damping (ξ) and m_e is an equivalent mass per unit length (for an uniform cylinder $m_e=m$).

The analysis assumes $\delta = 0.1$ as representative for oscillation in the first mode [9,10].

Table IV shows the Scruton number of stays and the size of lock-in region with reference to first in-plane vibration mode, evaluated according to [11]

$$U_{\text{lock,bot}} = 5.0 f_n D \qquad (16)$$

$$U_{\text{lock,top}} = 6.2 f_n D, \qquad (17)$$

demonstrating that lock-in is undoubtedly precluded and wind critical velocities are too low to generate vibrations.

TABLE IV. LOCK-IN REGION AND SCRUTON NUMBER OF STAYS

Stay	Yawing angle (°)	D (mm)	m (kg/m)	$f_{1,\text{in}}$ (Hz)	$U_{\text{lock,bot}}$ (m/s)	$U_{\text{lock,top}}$ (m/s)	Sc (–)
1	3.4	230	300	0.717	0.82	1.02	95
2	3.5	55	17	1.129	0.31	0.38	93
3	3.2	55	17	1.264	0.35	0.43	93
4	2.7	230	300	1.459	1.68	2.08	95
5	1.4	60	20	2.181	0.65	0.81	93
6	1.4	65	24	2.059	0.67	0.83	93
7	1.4	65	24	1.451	0.47	0.58	93
8	1.5	65	24	1.291	0.42	0.52	93
9	1.5	70	27	1.106	0.39	0.48	93
10	1.5	70	27	0.995	0.35	0.43	93
11	1.5	70	27	0.895	0.31	0.39	93
12	1.5	75	31	0.809	0.30	0.38	93
13	1.5	75	31	0.740	0.28	0.34	93
14	1.5	75	31	0.683	0.26	0.32	93
15	1.5	75	31	0.640	0.24	0.30	93
16	1.5	75	31	0.591	0.22	0.27	93
17	1.5	70	27	0.605	0.21	0.26	93

D. *Dry Inclined Galloping*

Dry inclined galloping is characterized by the occurrence of large amplitude motion and vibrations growing without bound, once the wind velocity exceeds the critical one [12]. This phenomenon is related to the appearance of an axial flow behind the cable, which velocity U_a increases with wind uniform velocity U and with the cable yawing angle. Instability appears when U_a>0.3 U for yawing angles greater than 25° [13]. More recently Matsumoto et al. [14] related dry inclined galloping to Kármán vortex mitigation and distinguished between divergent-type galloping (DIG) and unsteady galloping. The latter is characterized by unsteady and not so large vibration amplitude, so it might not interfere directly with the safety of inclined cables.

Experiments [15] and field observation [14] indicate that dry inclined galloping can be ignored for normally spaced cables (at least 10 D) with damping ratio ξ > 0.3% (external damped cables) which approximately corresponds to

$$Sc_0 = \frac{m\xi}{\rho D^2} > 3. \qquad (18)$$

E. *Rain Wind Induced Vibrations*

An exhaustive description of this phenomenon can be found in [1]. Designer wants to predict the occurrence of rain wind induced vibrations and set up counter-measures (for example, hydraulic dampers installed at cable ends). This can be achieved with the simplified model by Geurts and van Staalduinen [16]. They estimate the critical wind speed U_{cr} for rain wind induced vibrations and the maximum amplitude of vibration y_0 given by

$$U_{\text{cr}} = \frac{4m\xi\omega_e}{-\rho D\left(\frac{\mathrm{d}C_y}{\mathrm{d}\alpha} + C_D\right)} \qquad (19)$$

and

$$\left(\omega_e \frac{y_0}{U}\right)^2 = \frac{8}{\frac{\mathrm{d}^3 C_y}{\mathrm{d}\alpha'^3}}\left(-\frac{\mathrm{d}C_y}{\mathrm{d}\alpha'} - \frac{2\xi m\omega_e}{\frac{1}{2}\rho U D}\right) \qquad (20)$$

where ω_e is the natural circular frequency of cable in rad/s, and C_y is the coefficient for loading in the vertical direction and α' is the relative angle of attack. The authors adopt values of -0.8 and 54 for $\frac{\mathrm{d}C_y}{\mathrm{d}\alpha'}$ and $\frac{\mathrm{d}^3 C_y}{\mathrm{d}\alpha'^3}$ respectively. These key values result from wind tunnel test of a smooth cable model with an artificial upper rivulet.

According to [15] rain wind induced vibrations can be suppressed when

$$Sc_0 = \frac{m\xi}{\rho D^2} > 10 \qquad (21)$$

for stays with no surface treatments. The necessary damping ratio can be also obtained from (20), adopting appropriate limits for y_0, suitable to avoid alarming bridge users. It is reasonable to set $y_{0,\max} = D$; moreover, $y_{0,\max} = 0.5\ D$ make vibrations virtually unnoticeable [15]. For user comfort and safety, in Eurocode EN1993-1-11 the limit $y_{0,\max} = L/500$ is prosposed, instead, with a moderate wind velocity of 15 m/s, but for long stays this could result less restrictive.

Table V shows the damping requested for rain wind induced vibrations suppression in the stays of the considered bridge. In the table, case A ($\xi_{\text{req,A}}$) refers to (21), that is independent both on wind uniform velocity and on cable stay natural frequency; case B ($\xi_{\text{req,B}}$) refers to (20), assuming $y_{0,\max} = 0.5\ D$ and $U = 20$ m/s; this latter value derives from field observations, demonstrating that rain wind induced vibrations occur when the wind speed varies in the range (5÷20) m/s.

It can be highlighted, the design case B leads to less damping requirements for shorter stays (#3 to #10).

TABLE V. REQUESTED DAMPING FOR RAIN WIND INDUCED VIBRATIONS SUPPRESSION.

Stay	D (mm)	m (kg/m)	$\xi_{\mathrm{req,A}}$ (%)	$y_{0,\max}$ (m)	U_{m} (m/s)	ω_1 (rad/s)	$\xi_{1,\mathrm{req,B}}$ (%)	U_{cr} (m/s)
1	230	300	0.21	0.115	20	4.50	0.08	159
2	55	17	0.22	0.028	20	7.09	0.22	160
3	55	17	0.22	0.028	20	7.94	0.20	160
4	230	300	0.21	0.115	20	9.17	0.04	156
5	60	20	0.22	0.030	20	13.70	0.10	159
6	65	24	0.22	0.033	20	12.93	0.10	159
7	65	24	0.22	0.033	20	9.12	0.15	160
8	65	24	0.22	0.033	20	8.11	0.16	160
9	70	27	0.22	0.035	20	6.95	0.18	160
10	70	27	0.22	0.035	20	6.25	0.20	160
11	70	27	0.22	0.035	20	5.63	0.22	160
12	75	31	0.22	0.038	20	5.08	0.23	160
13	75	31	0.22	0.038	20	4.65	0.25	160
14	75	31	0.22	0.038	20	4.29	0.27	160
15	75	31	0.22	0.038	20	4.02	0.29	160
16	75	31	0.22	0.038	20	3.71	0.31	160
17	70	27	0.22	0.035	20	3.80	0.33	160

V. Concluding remarks

The relevant issue of vibration phenomena directly induced by wind in cable-stayed bridges has been presented and investigated for a significant case study. In particular, buffeting, von Kármán vortex-shedding, dry inclined galloping and rain wind induced vibrations have been considered and the required necessary damping has been evaluated.

The results show that for the stays of the considered bridge buffeting is a self-limiting phenomenon and vortex-shedding it is not relevant.

Instead a critical damping ratio of 0.3% on the first mode is obtained to control both dry inclined galloping and rain wind induced vibrations.

The obtained results are in good agreement with the actual requirements provided by EN1993-1-11 and by the Federal Highway Administration [15].

References

[1] E. de Sá Caetano, Cable Vibrations in Cable-Stayed Bridges. IABSE-AIPC-IVBH, 2007.

[2] J. Wianecki, "Cables wind excited vibrations of cable-stayed bridges," in 5th International Conference on Wind Engineering, pp. 1381–1393, 1979.

[3] Transportation Research Board and National Academies of Sciences, Engineering, and Medicine, "Inspection and Maintenance of Bridge Stay Cable Systems". Washington, D.C.: Transportation Research Board, 2005.

[4] J.P. Den Hartog; "Mechanical Vibrations", McGraw-Hill, New York, 1934.

[5] R. Castelluccio, "Il nuovo ponte strallato sull'Arno a Figline Valdarno," Università di Pisa, https://etd.adm.unipi.it/theses/available/etd-09082016-181846/, 2016.

[6] A. Mehrabi and H. Tabatabai, "Unified finite difference formulation for free vibration of cables," Journal of Structural Engineering, vol. 124, no. 11, pp. 1313–1322, 1998.

[7] H. M. Irvine, "Free Vibrations of Inclined Cables," Journal of the Structural Division, vol. 104, no. 2, pp. 343–347, 1978.

[8] W. Shi, C. Wang, D. Coles, and A. Roshko, "Experiments on flow past circular cylinders at large Reynolds numbers," Journal of Wind Engineering and Industrial Aerodynamics, vol. 49, pp. 348–351, 1993.

[9] H. Yamaguchi and Y. Fujino, "Stayed cable dynamics and its vibration control," in Bridge Aerodynamics, A. Larsen and S. Esdahl, Eds. Balkema, pp. 235–253, 1998.

[10] Y. Fujino, D. M. Siringoringo, T. Nagayama, and D. Su, "Control, simulation and monitoring of bridge vibration – Japan's recent development and practice," in IABSE-JSCE Joint Conference on Advances in Bridge Engineering-II, pp. 61–74, 2010.

[11] T. Sarpkaya, "A critical review of the intrinsic nature of vortex-induced vibrations," Journal of Fluids and Structures, vol. 19, pp. 389–447, 2004.

[12] G. Matteoni, C. T. Georgakis, F. Ricciardelli, M. Arentoft, H. Koss, and E. Svensson, "Understanding and simulating vibrations of plain bridge cables under varying meteorological conditions: Wind tunnel experimental work and analytical modelling," DTU Tryk, 2014.

[13] M. Matsumoto, "Observed behaviour of prototype cable vibration and its generating mechanism," in Bridge Aerodynamics, A. Larsen and S. Esdahl, Eds. Balkema, pp. 189–211, 1998.

[14] M. Matsumoto, T. Yagi, H. Hatsuda, T. Shima, M. Tanaka, and H. Naito, "Dry galloping characteristics and its mechanism of inclined/yawed cables," Journal of Wind Engineering and Industrial Aerodynamics, vol. 98, no. 6–7, pp. 317–327, 2010.

[15] S. Kumarasena, N. P. Jones, P. Irwin, and P. Taylor, Wind-Induced Vibration of Stay Cables. Federal Highway Administration, 2007.

[16] C. P. W. Geurts and P. C. van Staalduinen, "Estimation of the effects o rain-wind induced vibration in the design stage of inclined stay cables," presented at the Wind engineering into the 21st century, vol. 2, pp. 885–892, 1999.

[17] EN1993-1-11: "Eurocode 3: Design of steel structures - Part 1-11: Design of structures with tension components." CEN, Brussels, 2010.